

# Role of Water/Methanol Clustering Dynamics on Thermosensitivity of Poly(*N*-isopropylacrylamide) from Spectral and Calorimetric Insights

Shengtong Sun and Peiyi Wu\*

The Key Laboratory of Molecular Engineering of Polymers, Ministry of Education, Department of Macromolecular Science, and Laboratory of Advanced Materials, Fudan University, Shanghai 200433, People's Republic of China

Received July 25, 2010; Revised Manuscript Received September 25, 2010

**ABSTRACT:** The role of water/methanol clustering dynamics on thermosensitivity of poly(*N*-isopropylacrylamide) (PNIPAM) chains in concentrated solutions (10 wt %) is investigated by turbidity, FT-IR and calorimetric measurements through point-by-point comparison. FT-IR spectral variations show that PNIPAM–methanol interactions are largely weakened and PNIPAM chains are more collapsed in water/methanol mixture (methanol volume fraction  $x_m = 0.17$ ) than in pure water because of the formation of large water/methanol clusters, which, meanwhile, causes the decrease of hydration sites. On the other hand, weak hysteresis and excess recovery phenomena in the phase transition process can also be observed with addition of methanol to PNIPAM aqueous solution due to the existence of water/methanol clustering dynamics. Two-dimensional infrared correlation spectroscopy and calorimetric analysis finally conclude that the role of water/methanol clustering dynamics is mainly embodied in the inhibition of the hydration process of PNIPAM chains which shows a faster thermal response than hydrogen bonding association.

## 1. Introduction

Poly(*N*-isopropylacrylamide) (PNIPAM), as the most representative negatively thermo-responsive water-soluble polymer with a lower critical solution temperature (LCST,  $\sim 32^\circ\text{C}$ ), has been attracting much more attention for the past 2 decades.<sup>1</sup> Upon heating to above its LCST, the PNIPAM aqueous solution undergoes a coil-to-globule phase transition and can recover easily to the original state in the cooling process. Researches on the phase transition behavior of PNIPAM are very helpful to understand the nature of some life phenomena such as protein denaturation. The transition is generally related to be the competitive result of the hydrophobic interaction of pendent isopropyl groups and backbones and the hydrogen bonding association between amide groups and water molecules.<sup>2–5</sup>

Except for multiresponses to temperature,<sup>6</sup> pH,<sup>7</sup> ionic strength,<sup>8</sup> and pressure,<sup>9</sup> PNIPAM also shows unique sensitivity to solvent composition, such as water/alcohol,<sup>10–12</sup> water/DMF,<sup>13,14</sup> water/DMSO,<sup>15</sup> water/dioxane,<sup>16–18</sup> water/THF,<sup>19,20</sup> etc. However, the phase transition behavior of PNIPAM in water/methanol mixture<sup>21–31</sup> has been studied the most. Although water and methanol are both good solvents to PNIPAM, a proper mixture of them is a poor one. The LCST of PNIPAM in water/methanol mixture shifts to lower temperature from  $32^\circ\text{C}$  to a minimum value  $-7.5^\circ\text{C}$  as methanol volume fraction ( $x_m$ ) reaches 0.35, while a sharp increase occurs when  $x_m$  changes between 0.35 and 0.45 until total disappearance takes place for  $x_m > 0.45$ .<sup>21</sup> This phenomenon is known as typical LCST-type cononsolvency.<sup>12</sup> Therefore, if we continuously increase the methanol content at a constant temperature (e.g.,  $20^\circ\text{C}$ ), PNIPAM would undergo a reentrant coil-to-globule-to-coil phase transition,<sup>24,25,31</sup> which can even be used to purify PNIPAM in synthesis.<sup>32</sup> Interestingly, similar phenomena can also be found in water/organic solvent mixtures of poly(vinyl alcohol) (PVA),<sup>33</sup> poly(*N*-vinylpyrrolidone) (PVP),<sup>34–36</sup>

poly(*N*-vinylcaprolactam) (PVCL),<sup>36</sup> poly(vinyl methyl ether) (PVME),<sup>22,37</sup> poly(*N,N*-dimethylacrylamide) (PDMAM),<sup>38</sup> poly(*N*-(2-ethoxyethyl)acrylamide) (PEoEA),<sup>39</sup> poly(*N,N*-diethylacrylamide) (PDEA)<sup>40</sup> as well as other oligomeric polyacrylamides.<sup>41</sup>

Up to the present, plenty of investigations have been devoted to elucidate the nature of cononsolvency of PNIPAM in water/methanol mixture, including some structurally confined systems, e.g., PNIPAM gels,<sup>42–46</sup> PNIPAM brushes<sup>47</sup> and interfaces.<sup>48,49</sup> However, the origin of the reentrant transition of PNIPAM has still not been well established. Preferential absorption of methanol on PNIPAM<sup>50</sup> has ever been proposed to account for this phenomenon, which, however, cannot be adequately supported by either experimental<sup>23</sup> or simulation<sup>31</sup> results. Thus a mechanism involving competitive hydrogen bonding by water and methanol molecules onto the polymer chain was put forward.<sup>28,30</sup> On the other hand, water/methanol complexation, the simplest hydrophilic–hydrophobic pair, has been investigated extensively for more than 70 years. Especially, more and more recent studies have provided evidence for the immiscibility of the water/alcohol solution on a microscopic scale.<sup>51–54</sup> On the basis of this point, a more acceptable mechanism was proposed by Zhang and Wu that the reentrant coil-to-globule-to-coil transition behavior can be attributed to the formation of different water/methanol clusters,  $(\text{H}_2\text{O})_m(\text{CH}_3\text{OH})_n$ , which are poor solvents to PNIPAM,<sup>24,25</sup> although the geometry of water/methanol clusters is rather hard to be confirmed. Recently, Yang and Ma et al. revealed by molecular dynamics simulation that NIPAM–solvent interactions are weakened with the increase of methanol, which commendably supported the above mechanism.<sup>31</sup>

As we know, IR is rather sensitive to morphology and conformational changes by reflecting subtle information at molecular level. Up to now, a few FTIR studies have been reported on the reentrant phase transition behavior of PNIPAM in water/methanol mixture, indicating that both hydrophobic isopropyl and backbone C–H groups and hydrophilic amide groups are contributing to the reentrant transition behavior.<sup>10,55,56</sup>

\*Corresponding author. E-mail: peiyiwu@fudan.edu.cn.

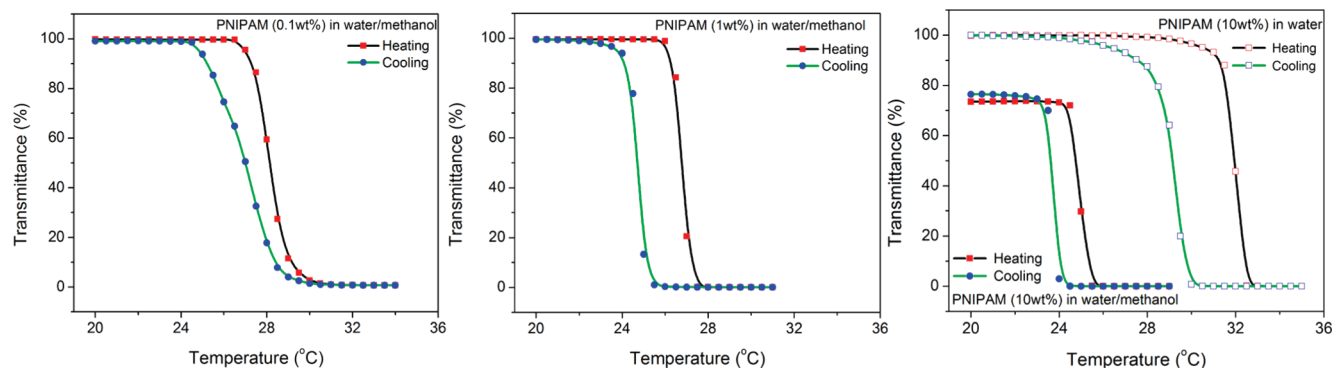


**Figure 1.** Temperature dependent transmittance of 0.1, 1, 10 wt % PNIPAM solutions in water/methanol mixture and 10 wt % PNIPAM in pure water during heating and cooling cycles with an increment of 0.5 °C.

However, nearly all the previous researches were focused on the phase transition behavior of PNIPAM induced by solvent composition, whereas no investigations of the effect of methanol on thermosensitivity of PNIPAM in this binary solvents have ever been reported, which is also very helpful to understand the nature of cononsolvency phenomenon. In this paper, we present our results of point-by-point spectral comparison combined with turbidity and calorimetric analysis of the thermally induced phase transition behavior of PNIPAM in water/methanol mixture with that in pure water. Wherein, the existence of water/methanol clusters can be further confirmed and the great influence of their clustering dynamics on thermosensitivity of PNIPAM will be elucidated.

## 2. Experimental Section

**2.1. Materials.** *N*-Isopropylacrylamide (NIPAM) was purchased from Tokyo Kasei Kogyo Co. (Tokyo, Japan) and recrystallized from cyclohexane before use. Azobis(isobutyronitrile) (AIBN) was purchased from aladdin reagent Co. and recrystallized from ethanol. THF was vacuum distilled from calcium hydride before use. PNIPAM was synthesized by radical polymerization in THF using AIBN as an initiator. After three freeze–pump–thaw cycles, the polymerization reaction proceeded at 60 °C for 18 h under nitrogen protection. The synthesized polymer was purified by reprecipitation in diethyl ether twice and further vacuum-dried for 24 h. The number average molecular weight of PNIPAM,  $M_n = 1.4 \times 10^5$  and polydispersity index  $M_w/M_n = 1.80$  was determined by GPC measurements with monodisperse polystyrene as standard and THF as eluent phase at 35 °C.

D<sub>2</sub>O and CD<sub>3</sub>OD were purchased from Cambridge Isotope Laboratories Inc. (D-99.9%). The concentration of PNIPAM was fixed to 0.1, 1, and 10 wt % respectively for comparison in turbidity measurements. For FT-IR and calorimetric measurements, the concentration of PNIPAM in water/methanol mixtures and in pure water was all fixed to 10 wt %.

Unless stated otherwise, the methanol volume fraction ( $x_m$ ) in water/methanol mixtures was fixed to 0.17 with a 5:1 volume ratio. All PNIPAM solutions in D<sub>2</sub>O and in D<sub>2</sub>O/CD<sub>3</sub>OD mixtures were placed at 4 °C for a week before FTIR measurements to ensure complete deuteration of all the N–H protons.

**2.2. Instruments and Measurements.** Calorimetric measurements were performed on a Mettler-Toledo differential scanning calorimeter thermal analyzer. Turbidity measurements were made at 500 nm on a Lamda 35 UV–vis spectrometer with pure water as reference (100% transmittance) without stirring. Temperatures were manually ramped with a water-jacketed cell holder at rates of ca. 0.5 °C/min with an increment of 0.5 °C. Each temperature point was maintained for one minute to ensure thermal equilibrium of the sample cell (quartz glass). The sample of PNIPAM solution for FT-IR measurements was prepared by being sealed between two CaF<sub>2</sub> tablets. All time-resolved FT-IR spectra at different

temperatures were recorded on a Nicolet Nexus 470 spectrometer with a resolution of 4 cm<sup>−1</sup>, and 32 scans were available for an acceptable signal-to-noise ratio. Temperatures were manually controlled with an electronic cell holder at rates of ca. 0.3 °C/min with an increment of 0.5 °C. Raw spectra were baseline-corrected by the software Omnic, ver. 6.1a.

**2.3. Investigation Methods.** **2.3.1. Perturbation Correlation Moving Window (PCMw).** FT-IR spectra collected with an increment of 0.5 °C during heating and cooling were used to perform 2D correlation analysis, respectively. Primary data processing was carried out with the method Morita provided and further correlation calculation was performed using the software 2D Shige, ver. 1.3 (Shigeaki Morita, Kwansei-Gakuin University, Japan, 2004–2005). The final contour maps were plotted by Origin program, ver. 8.0, with warm colors (red and yellow) defined as positive intensities and cool colors (blue) as negative ones. An appropriate window size ( $2m + 1 = 11$ ) was chosen to generate PCMw spectra with good quality.

**2.3.2. 2D Correlation Spectroscopy (2Dcos).** FT-IR spectra used for PCMw analysis were also used to perform 2D correlation analysis. 2D correlation analysis was carried out using the same software 2D Shige ver. 1.3 (Shigeaki Morita, Kwansei-Gakuin University, Japan, 2004–2005), and was further plotted into the contour maps by Origin program ver. 8.0. In the contour maps, warm colors (red and yellow) are defined as positive intensities, while cool colors (blue) are defined as negative ones.

## 3. Results and Discussion

**3.1. Turbidity Measurements.** The phase transition behavior of PNIPAM in water/methanol mixture was first examined by turbidity measurement. Note that a proper 5:1 volume ratio of water/methanol mixture is chosen in this paper which has caused a certain decrease of the LCST of PNIPAM aqueous solution while the effect of methanol could also be elegantly embodied. For comparison, both the methanol effect and concentration effect on phase transition behavior of PNIPAM during heating and cooling cycles are characterized by measuring the change of transmittance with an increment of 0.5 °C, as shown in Figure 1.

LCSTs were taken as the initial break points in the resulting optical density versus temperature curves. Thus LCSTs of 10 wt % PNIPAM in water/methanol and in pure water during heating can be easily determined to be 24.5 and 31.5 °C, while those of them during cooling to be 24 and 30 °C, respectively. The addition of methanol ( $x_m = 0.17$ ) leads to ca. 6–7 °C decrease of the LCST of PNIPAM aqueous solution by turbidity measurements. Interestingly, the hysteresis of 10 wt % PNIPAM in water/methanol mixture (0.5 °C) is a little weaker than that of PNIPAM in pure

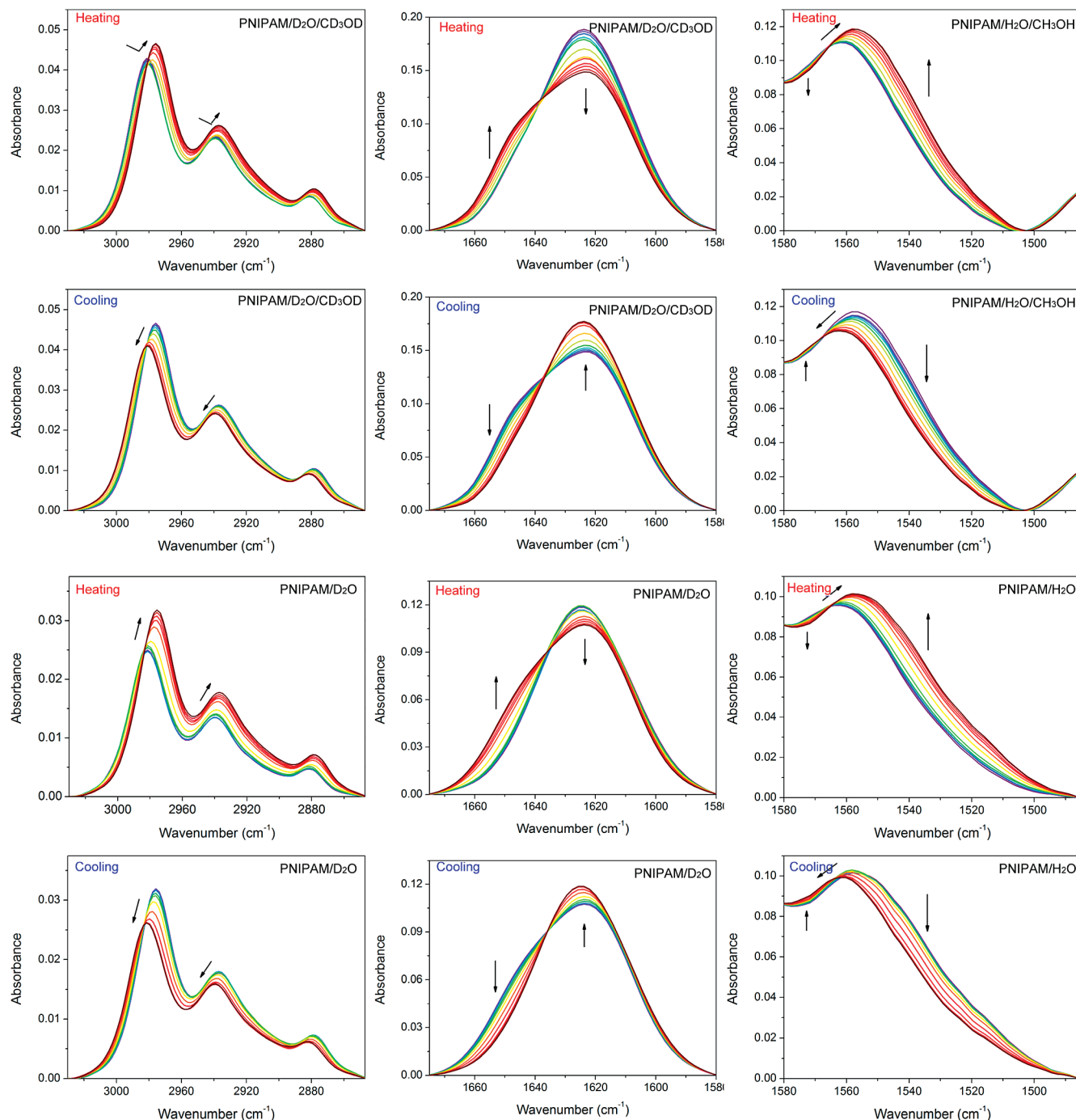


**Figure 2.** Temperature dependent FT-IR spectra of 10 wt % PNIPAM solutions in 5:1 water/methanol mixture (22–33 °C) and in pure water (28–38 °C) during heating and cooling. For clarity, only spectra at intervals of 1 °C are shown here.

water (1.5 °C). Furthermore, the initial transmittance of PNIPAM in water/methanol mixture at lower temperature before phase separation is rather lower than that of PNIPAM in pure water, indicating much higher degree of chain collapse or dehydration of PNIPAM due to the addition of methanol. On the other hand, if we examine the transmittance variations carefully, we can find an excess recovery phenomenon after a heating and cooling cycle in PNIPAM/water/methanol solution, which, however, cannot be detected in PNIPAM aqueous solution.

However, in dilute and semidilute conditions (0.1 and 1 wt %), the addition of methanol does not induce large decrease of initial transmittance of PNIPAM aqueous solutions, and the excess recovery phenomenon cannot be observed either.

Weak hysteresis also exists in dilute and semidilute PNIPAM solutions, but the recovery process during cooling slowed down in 0.1 wt % concentration; in other words, the recovery process was accelerated by the addition of methanol especially in concentrated PNIPAM aqueous solutions, which may also be the reason for weak hysteresis. The combining methanol and concentration effect on weak hysteresis and excess recovery phenomena of PNIPAM in water/methanol mixture will be further discussed in the following FTIR analysis.

**3.2. Conventional IR Analysis.** Due to apparent weak hysteresis and excess recovery phenomena in concentrated PNIPAM solutions, temperature-dependent FT-IR measurements of 10 wt % PNIPAM in water/methanol mixture



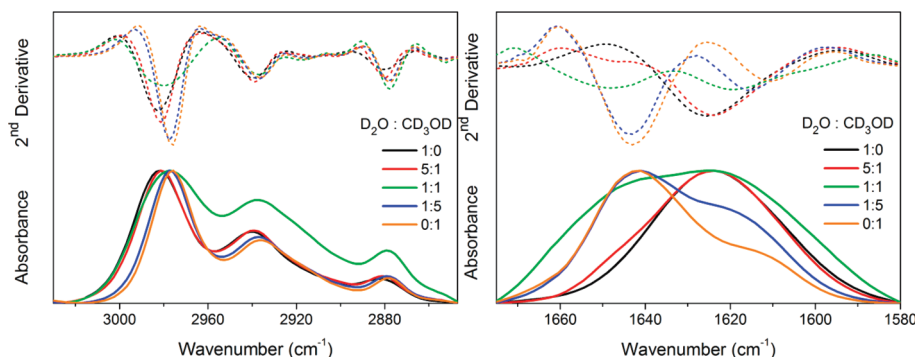


**Figure 3.** FT-IR and corresponding second derivate spectra of 10 wt % PNIPAM in water/methanol mixtures of different volume ratios ( $\text{D}_2\text{O}:\text{CD}_3\text{OD} = 1:0, 5:1, 1:1, 1:5$  and  $0:1$ ) at  $22^\circ\text{C}$ .

(5:1 volume ratio) and in pure water were performed during heating and cooling, as presented in Figure 2. Three regions are focused in this paper: C–H stretching region ( $3030\text{--}2847\text{ cm}^{-1}$ ), amide I ( $\text{C}=\text{O}$  stretching,  $1675\text{--}1580\text{ cm}^{-1}$ ) as well as amide II ( $\text{N}\text{--}\text{H}$  bending,  $1580\text{--}1485\text{ cm}^{-1}$ ), which can be used to trace all group motions of PNIPAM in the reversible phase transition process. For C–H and  $\text{C}=\text{O}$  stretching region, it should be noted that we used  $\text{D}_2\text{O}$  and  $\text{CD}_3\text{OD}$  instead of  $\text{H}_2\text{O}$  and  $\text{CH}_3\text{OH}$  as the solvent here in order to eliminate the overlap of  $\delta(\text{O}\text{--}\text{H})$  band around  $1640\text{ cm}^{-1}$  with  $\nu(\text{C}=\text{O})$  of PNIPAM as well as the broad  $\nu(\text{O}\text{--}\text{H})$  band around  $3300\text{ cm}^{-1}$  with  $\nu(\text{C}\text{--}\text{H})$  bands of PNIPAM.<sup>5</sup> As reported, the transition temperature of PNIPAM in  $\text{D}_2\text{O}$  is  $0.7^\circ\text{C}$  higher than that in  $\text{H}_2\text{O}$ . However, the deuterium isotope effect does not cause obvious changes on the magnitude of hysteresis.<sup>57,58</sup> Meanwhile, in spite of partially overlapping with  $\delta(\text{O}\text{--}\text{H})$ , amide II can still be resolved in  $\text{H}_2\text{O}/\text{CH}_3\text{OH}$  and  $\text{H}_2\text{O}$  solutions.<sup>59</sup> Whereas, the original spectra should be pretreated by a single point baseline correction combined with subsequent normalization at  $1580\text{ cm}^{-1}$  to avoid the effect of  $\delta(\text{O}\text{--}\text{H})$ .

Examine the spectral variations of PNIPAM in water/methanol mixture and in pure water during heating and cooling in Figure 2, surprisingly, we cannot find any new bands or large different spectral changes between these two systems. It seems that in 5:1 water/methanol mixture, PNIPAM-methanol interactions are largely weakened. To confirm our supposition, FT-IR spectra of 10 wt % PNIPAM in water/methanol of other three volume ratios were also collected for comparison at  $22^\circ\text{C}$ , as shown in Figure 3. Note that at  $22^\circ\text{C}$  PNIPAM chains in 1:1  $\text{CD}_3\text{OD}/\text{D}_2\text{O}$  mixture are in collapsed state due to rather lower LCST than room temperature and all IR bands are relatively broad. As the volume fraction of methanol increases, both CH and amide I bands shift largely to lower wavenumbers, even more than  $10\text{ cm}^{-1}$  for  $\nu_{\text{as}}(\text{CH}_3)$  and amide I. However, after addition of small fraction of methanol such as 5:1 volume ratio of  $\text{D}_2\text{O}/\text{CD}_3\text{OD}$  mixture studied in this paper, the wavenumber shift of PNIPAM is rather low (about  $1\text{--}2\text{ cm}^{-1}$ ), which may only arise from the difference of chain collapse degree of PNIPAM chains. It is especially worth noting that FT-IR spectra of 2 wt % PNIPAM in water/methanol mixtures do not show significant wavenumber shift with addition of methanol as previously reported.<sup>56</sup> It is presumed that the reentrant phase transition behavior may also be related to the concentration of PNIPAM, which still needs further investigations.

The weak PNIPAM–methanol interaction can be easily understood if methanol formed large clusters with massive water molecules making it hard to contact by PNIPAM chains. On the other hand, the formation of water/methanol

clusters dispersed in pure water molecules and clusters would lead to the decrease of hydration sites of PNIPAM, which can also explain the decrease of LCST and the increase of degree of chain collapse observed in turbidity measurement. In other words, the water-PNIPAM interactions are also weakened due to the formation of water/methanol clusters, in conformity with previous experimental and molecular simulation results.<sup>24,25,31</sup>

Now we come back to spectral variations in Figure 2. It is notable that a slight difference of spectral variation trends can be observed between these two solutions. That is, the  $\nu_{\text{as}}(\text{CH}_3)$  band around  $2980\text{ cm}^{-1}$  has a slight intensity decrease before phase transition during heating along with an obvious frequency shift. Interestingly, PNIPAM gel and concentrated PNIPAM aqueous solution also exhibit similar intensity changes,<sup>60</sup> indicating that the addition of methanol leads to somehow constraint of PNIPAM chains, corresponding to the increase of degree of chain collapse.

No matter for PNIPAM in water/methanol mixture or for PNIPAM in pure water, three regions show similar changes: during heating, C–H stretching bands all shift to lower frequencies, which can be attributed to the dehydration process of hydrophobic groups in PNIPAM chains;<sup>61</sup>  $\text{C}=\text{O}$  stretching bands exhibit a binary spectral intensity changes, arising from the transformation from  $\text{C}=\text{O}\cdots\text{D}_2\text{O}$  hydrogen bonds ( $1625\text{ cm}^{-1}$ ) to  $\text{C}=\text{O}\cdots\text{D}\text{--}\text{N}$  ones ( $1651\text{ cm}^{-1}$ );<sup>16,62</sup> Amide II show both a frequency shift and a binary intensity change, corresponding to the conversion between  $\text{N}\text{--}\text{H}\cdots\text{H}_2\text{O}$  ( $1572\text{ cm}^{-1}$ ) and  $\text{N}\text{--}\text{H}\cdots\text{O}=\text{C}$  hydrogen bonds ( $1543\text{ cm}^{-1}$ ).<sup>55,59</sup> For the convenience of comparison, three spectra of PNIPAM solutions in water/methanol and in pure water at three same temperatures are shown in Figure 4. Apparently, the addition of methanol causes the further dehydration of C–H groups, the increase of  $\text{C}=\text{O}\cdots\text{H}(\text{D})\cdots\text{N}$  hydrogen bonds and the decrease of hydrogen bonds between amide groups and water molecules. It can also be attributed to the decrease of hydration sites of PNIPAM chains due to the formation of large water/methanol clusters.

As we know, the water–methanol clusters have different stability at different temperatures, thus an association-dissociation process can be expected during heating and cooling. The question is, does water–methanol clustering process have any influence on the phase transition of PNIPAM in water/methanol mixture? To investigation this effect, the frequency shifts of  $\nu_{\text{as}}(\text{CH}_3)$ ,  $\nu_{\text{as}}(\text{CH}_2)$ , and amide II as well as the content changes of hydrated/dehydrated  $\text{CH}_3$  groups and hydrogen bonds of amide I groups are plotted in Figure 5 and 6, respectively. Note that the content changes of hydrated/dehydrated  $\text{CH}_3$  groups are roughly reflected by intensity changes at  $2990$  and  $2970\text{ cm}^{-1}$  read from later PCMW and 2Dcos synchronous spectra, while

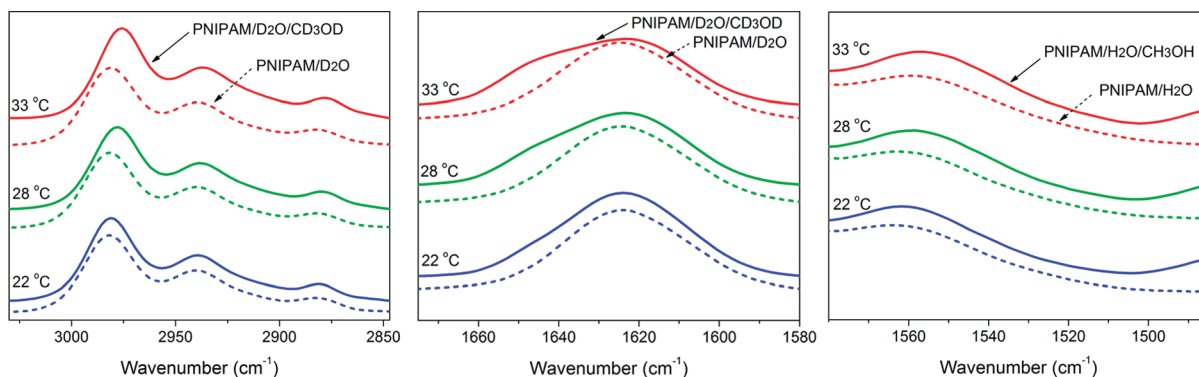


**Figure 4.** Spectral comparison between 10 wt % PNIPAM solutions in 5:1 water/methanol mixture (solid lines) and in pure water at three same temperatures during heating (dashed lines).

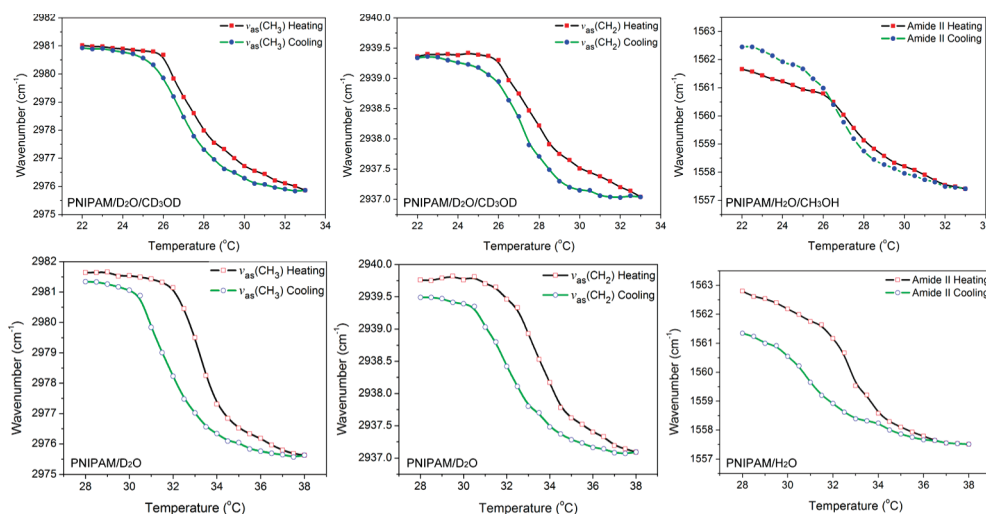


**Figure 5.** Temperature dependent frequency shifts of  $\nu_{as}(\text{CH}_3)$ ,  $\nu_{as}(\text{CH}_2)$  and amide II of 10 wt % PNIPAM in 5:1 water/methanol mixture (top) and in pure water (bottom) during heating and cooling.

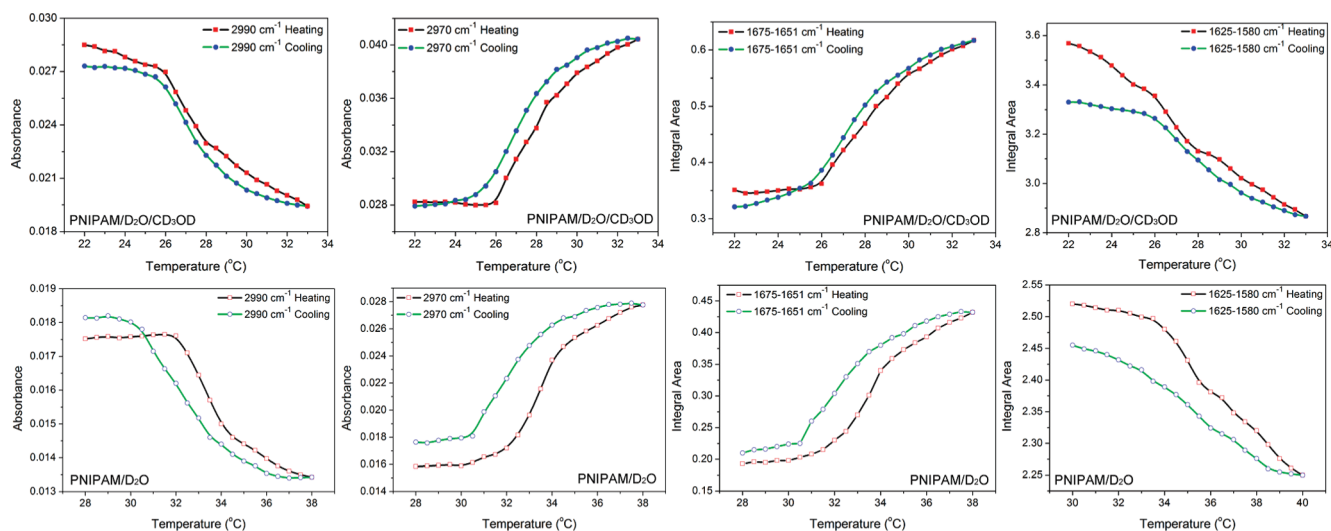


**Figure 6.** Temperature dependent content changes of hydrated/dehydrated  $\text{CH}_3$  groups and hydrogen bonds of amide groups of 10 wt % PNIPAM in 5:1 water/methanol mixture (top) and in pure water (bottom) during heating and cooling.

those of hydrogen bonds of amide I groups are represented by partial integral area.

Interestingly, similar weak hysteresis and excess recovery phenomena of PNIPAM in water/methanol mixture can also be observed either for frequency changes or for content

changes, especially for dehydrated  $\text{CH}_3$  ( $2970\text{ cm}^{-1}$ ) and  $\text{C=O}\cdots\text{D-N}$  hydrogen bonds ( $1675\text{--}1651\text{ cm}^{-1}$ ), which are both related to the collapsed state of PNIPAM chains. It can be interpreted that the globule-to-coil transition of PNIPAM aqueous solution during cooling was accelerated by the

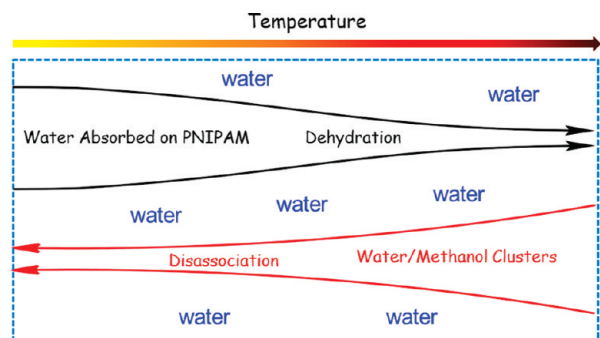


**Figure 7.** Illustration of the hydration-dehydration process of PNIPAM in water/methanol mixture and the association-disassociation process of water/methanol clusters. Wherein, the arrow indicates the release of water molecules.

addition of methanol in conformity with turbidity analysis and this effect cannot be immediately eliminated after the heating and cooling cycle. It is presumed that this accelerating effect may come from the water–methanol clustering process. According to previous NMR results, water–methanol clusters are more stable at high temperature, whereas, upon cooling to low temperature, more clusters of single species are present in the mixture.<sup>63</sup> Furthermore, the relaxation time of water–methanol clusters are faster than those of pure water and methanol, or in other words, water–water hydrogen bonds are longer lived than water–methanol clusters, resulting in an enhanced segregation as the mixtures are cooled.<sup>63–65</sup> This behavior is much more like an “upper critical solution temperature” (UCST)-type phase transition with the transition point “hidden” below the freezing line.<sup>65</sup>

Therefore, the effect of association-disassociation of water/methanol clusters on the content of water in mixtures is just contrary to that of dehydration-hydration during heating and cooling. In other words, the role of water/methanol clustering is much like a “reservoir”. During cooling, much more water is released from the disassociation process of water–methanol clusters to hydrate PNIPAM chains, resulting in the acceleration of the globule-to-coil phase transition. For the convenience of comprehension, these two processes have been illustrated in Figure 7.

As former turbidity analysis shows, increasing the concentration of PNIPAM in water/methanol mixtures is also favorable for the accelerating effect in the cooling process. As we know, increasing the concentration of PNIPAM consequently leads to the increase of entanglement density of polymer chains, while the diffusion of small molecules such as water, methanol and their clusters would be restricted to a certain extent. An extreme example is cross-linked PNIPAM hydrogel, in which the diffusion process cannot be neglected in chain collapse and swelling processes.<sup>60,66</sup> Therefore, it is much easier for water molecules just released from water–methanol clusters to hydrate PNIPAM chains before self-associating via hydrogen bonding due to the local microenvironment brought by the increase of PNIPAM concentration. Thus the accelerating effect of increasing PNIPAM concentration can also be explained.

### 3.3. Perturbation Correlation Moving Window Analysis.

To determine the LCST of PNIPAM in water/methanol mixture more accurately, PCMW technique was employed. PCMW is a newly developed technique, whose basic principles can date back to conventional moving window proposed by Thomas,<sup>67</sup> and later in 2006 Morita<sup>68</sup> improved

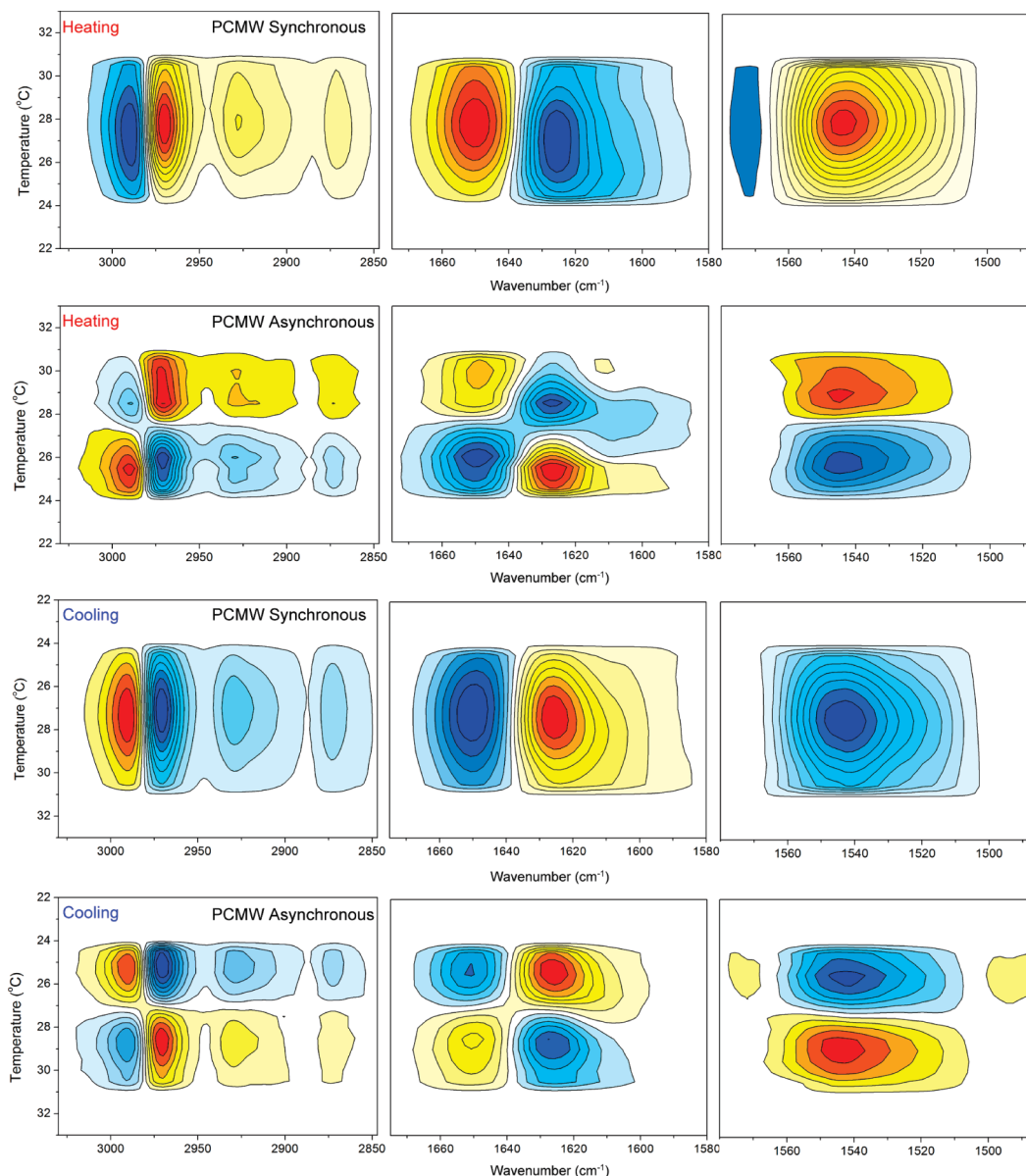
this technique to much wider applicability through introducing the perturbation variable into correlation equation. Except for its original ability in determining drastic change points as conventional moving window did, PCMW can additionally monitor complicated spectral variations along the perturbation direction. The rules of PCMW can be summarized as follows: positive synchronous correlation represents spectral intensity increasing, while negative one represents decreasing; positive asynchronous correlation can be observed for a convex spectral intensity variation while negative one can be observed for a concave variation.<sup>68</sup>

Figure 8 presents PCMW synchronous and asynchronous spectra of PNIPAM in water/methanol mixture between 22 and 33 °C during heating and cooling. PCMW synchronous spectra can be used to find drastic spectral change points, which can be interpreted as phase transition temperatures in this system, while asynchronous spectra can be used to determine the phase transition temperature range according to the turning points in the contour maps. For convenience, the results of LCSTs and transition temperature ranges arising from different vibrational bands determined by PCMW are listed in Table 1. Obviously, the LCSTs and transition temperature ranges during heating and cooling are very close to each other, not excluding some anomalous points, strongly indicating the weak hysteresis of PNIPAM in water/methanol mixture.

**3.4. 2D Correlation Analysis.** Now that we have confirmed the water/methanol clustering dynamics to be the reason of weak hysteresis and excess recovery phenomena in PNIPAM/water/methanol solution, we still wonder which process in the phase transition is mostly influenced by the water/methanol clustering dynamics. Is the hydration process or hydrogen bonding association? To solve this problem, 2Dcos was performed in this paper.

2Dcos is a mathematical method whose basic principles were first proposed by Noda in 1986.<sup>69</sup> Up to the present, 2Dcos has been widely used to study spectral variations of different chemical species under various external perturbations (e.g., temperature, pressure, concentration, time, electromagnetic, etc.).<sup>70</sup> Due to different responses of different species to external variable, additional useful information about molecular motions or conformational changes can be extracted which cannot be obtained straight from conventional 1D spectra. The judging rule can be summarized as Noda’s rule—that is, if the cross-peaks ( $\nu_1$ ,  $\nu_2$ , and assume  $\nu_1 > \nu_2$ ) in synchronous and asynchronous spectra have the same sign, the change at  $\nu_1$  may occur prior to that of  $\nu_2$ , and vice versa.

On the basis of transition temperature regions obtained from PCMW, we chose all the spectra between 27 and 31 °C to perform 2Dcos analysis, as shown in Figure 9. According to Noda’s rule, the sequence orders among C–H, amide I and amide II of PNIPAM in water/methanol mixture during heating and cooling can be deduced, as shown in Table 2. Corresponding order of PNIPAM in pure water<sup>5</sup> are also presented here for comparison. Note that the sequence orders of PNIPAM in pure water during heating and cooling are opposite to each other, indicating good reversibility of phase transition behavior. However, the orders of PNIPAM in water/methanol mixture during heating and cooling are both lead by amide I, while C–H related changes or hydration process are inhibited. It suggests that the existence of water/methanol clustering dynamics has positive effect on hydrogen bonding association



**Figure 8.** PCMW synchronous and asynchronous spectra of 10 wt % PNIPAM in 5:1 water/methanol mixture generated from all spectra between 22 and 33 °C during heating (top) and cooling (bottom). Wherein, warm colors (red and yellow) are defined as positive intensities, while cool colors (blue) as negative ones.

**Table 1.** LCSTs and Transition Temperature Ranges Arising from Different Vibration Bands Determined by PCMW

frequency/cm <sup>-1</sup>	heating		cooling	
	LCST/°C	transition range/°C	LCST/°C	transition range/°C
2990	29.5	27.5–30.5	29.5	27.0–30.5
2970	30.0	28.0–31.5	29.0	27.0–30.5
2927	30.0	28.0–31.5	29.0	27.0–30.5
2872	30.0	28.0–31.5	29.0	27.0–30.5
1651	30.0	28.0–31.5	29.0	27.5–30.5
1625	29.0	27.5–30.5	29.5	27.5–30.5
1543	30.0	27.5–31.0	29.5	27.5–31.0

or negative effect on hydration process. It may be arising from the fact that the relaxation time of dynamic hydration process of hydrophobic groups is shorter than the association process of relatively stronger hydrogen bonds, which, meanwhile, is less influenced by water/methanol clustering dynamics.

**3.5. Calorimetric Measurements.** Calorimetric method was also used to further confirm the existence of water/

methanol clustering dynamics and examine its influence on different processes of phase transition. Assuming the water/methanol clustering dynamic process always needs a period of time to approach a steady state, we may detect this process by changing annealing time after the first heating procedure at a proper scanning rate. Three groups of DSC curves at different scanning rates of 10 wt % PNIPAM in 5:1 water/methanol mixture and in pure water



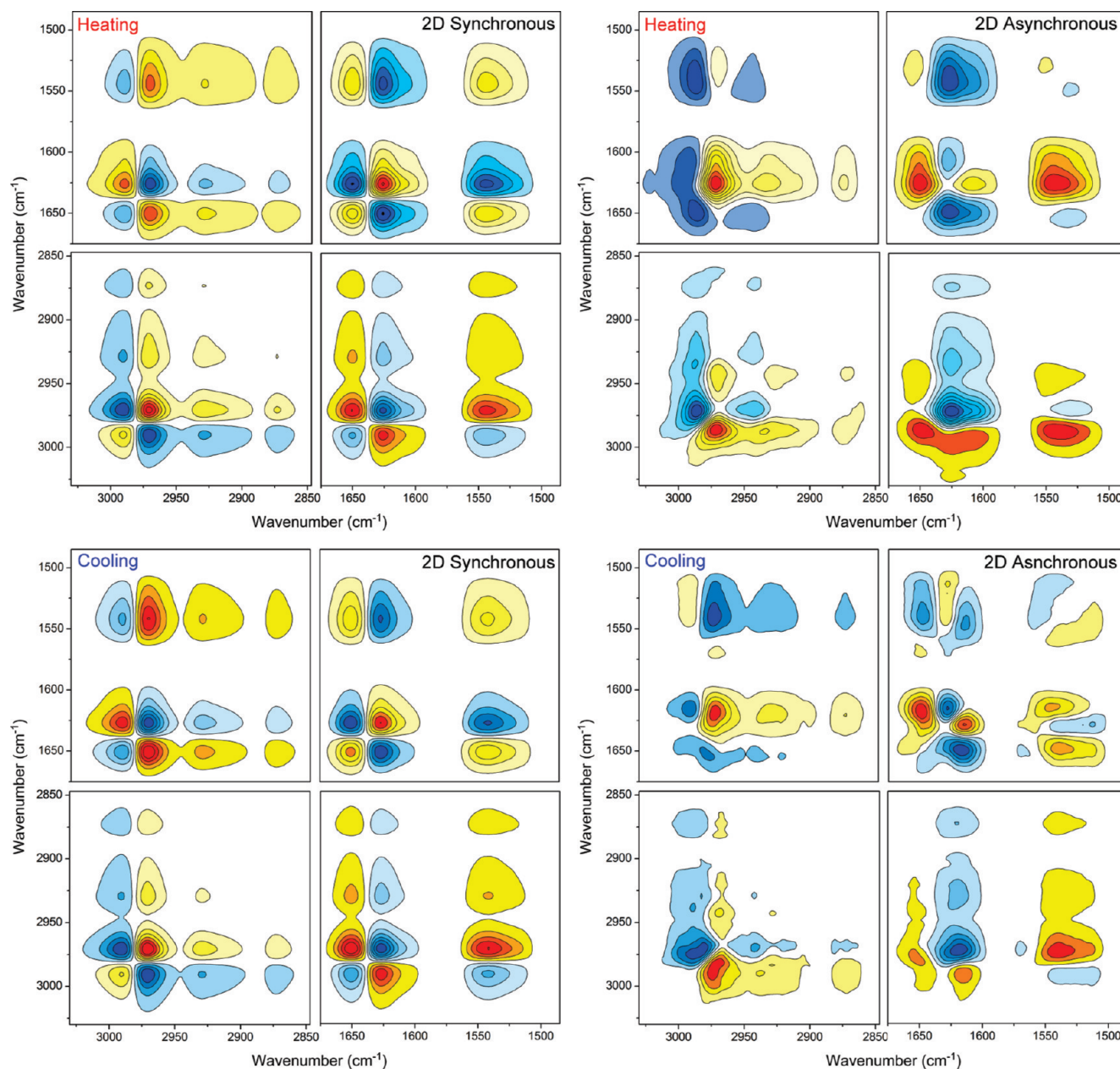


**Figure 9.** 2D synchronous and asynchronous spectra of 10 wt % PNIPAM in 5:1 water/methanol mixture generated from all spectra between 27 and 31 °C during heating (top) and cooling (bottom). Herein, warm colors (red and yellow) are defined as positive intensities, while cool colors (blue) are defined as negative ones.

**Table 2.** Sequence Orders among C–H, Amide I, and Amide II of PNIPAM in Water/Methanol Mixture and in Pure Water during Heating and Cooling (→ Means Prior to)

	PNIPAM/water/methanol	PNIPAM/water
heating	amide I → Amide II → C–H	C–H → amide II → Amide I
cooling	Amide I → C–H → amide II	Amide I → amide II → C–H

by changing annealing time are presented in Figure 10. From Figure 10, it is noted that faster scanning rate leads to higher transition temperature ( $T_p$ ) during heating and lower  $T_p$  during cooling, either for PNIPAM in methanol/water mixture or for PNIPAM in pure water, indicating that  $T_p$  here is not the transition temperature in equilibrium.<sup>6</sup> It should also be noted that a transition with two asymmetric exothermic peaks is observed during cooling. Considering there are still no acceptable explanations of these two peaks for concentrated PNIPAM

aqueous solutions in which interactions among polymer chains cannot be neglected, we tentatively attribute the two peaks located at higher and lower temperatures to the disruption of additional hydrogen bonding and the dissolution or hydration of collapsed chains respectively which was concluded from dilute conditions at rather low cooling rates.<sup>6</sup> Compared to PNIPAM in pure water, the peak at lower temperature was strongly suppressed with the addition of methanol. In addition, as expected, for PNIPAM in water/methanol mixture, extending annealing time at a relatively faster scan rate resulted in the enthalpy increase of the peak at lower temperature and the enthalpy decrease of the peak at higher temperature. In other words, from calorimetric measurements, we came to the same conclusion as 2Dcos analysis that the hydration process of PNIPAM chains is inhibited with the addition of methanol.



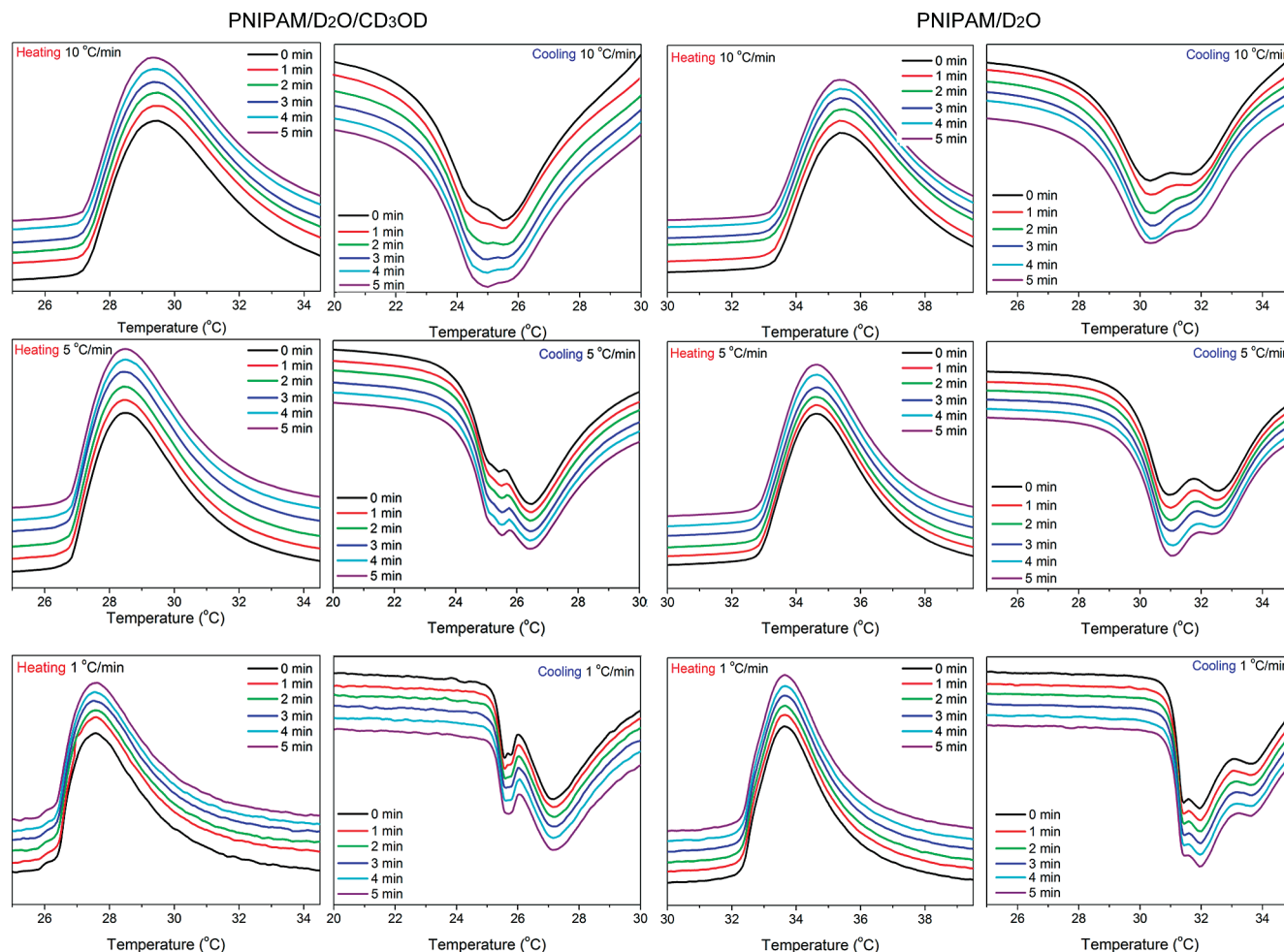


**Figure 10.** DSC curves at different scanning rates (1, 5, 10 °C/min) of 10 wt % PNIPAM in 5:1 water/methanol mixture and in pure water by changing annealing time (1–5 min).

#### 4. Conclusion

In this paper, turbidity, FT-IR and calorimetric measurements are employed to elucidate the role of water/methanol clustering dynamics on thermosensitivity of PNIPAM in concentrated solutions (10 wt %) through point-by-point comparison of the phase transition behavior of PNIPAM in water/methanol mixture and in pure water. Turbidity results show weak hysteresis and excess recovery phenomena of the phase transition with addition of methanol (methanol volume fraction  $x_m = 0.17$ ), which can also be confirmed by conventional IR and PCMW analysis. IR spectral variations reveal that PNIPAM-methanol interactions are largely weakened, and PNIPAM chains are more collapsed in water/methanol mixture than in pure water due to the formation of large water/methanol clusters, which, meanwhile, leads to the decrease of hydration sites. The role of water/methanol clustering dynamics is mainly embodied in the inhibition of the hydration process of PNIPAM chains confirmed by 2Dcos and calorimetric results. Moreover, the reentrant phase transition behavior may also be related to the concentration of PNIPAM according to our analysis, which still needs further investigations.

**Acknowledgment.** We gratefully acknowledge the financial support National Science Foundation of China (NSFC) (20934002, 20774022), the National Basic Research Program of China (No. 2009CB930000).

#### References and Notes

- (1) Schild, H. G. *Prog. Polym. Sci.* **1992**, *17*, 163.
- (2) Ono, Y.; Shikata, T. *J. Am. Chem. Soc.* **2006**, *128*, 10030.
- (3) Ye, X.; Lu, Y.; Shen, L.; Ding, Y.; Liu, S.; Zhang, G.; Wu, C. *Macromolecules* **2007**, *40*, 4750.
- (4) Zhou, K.; Lu, Y.; Li, J.; Shen, L.; Zhang, G.; Xie, Z.; Wu, C. *Macromolecules* **2008**, *41*, 8927.
- (5) Sun, B.; Lin, Y.; Wu, P.; Siesler, H. *Macromolecules* **2008**, *41*, 1512.
- (6) Ding, Y.; Ye, X.; Zhang, G. *Macromolecules* **2005**, *38*, 904.
- (7) Al-Manasir, N.; Zhu, K.; Kjøniksen, A.-L.; Knudsen, K. D.; Karlsson, G.; Nyström, B. *J. Phys. Chem. B* **2009**, *113*, 11115.
- (8) Zhang, Y.; Foryk, S.; Bergbreiter, D. E.; Cremer, P. S. *J. Am. Chem. Soc.* **2005**, *127*, 14505.
- (9) Meersman, F.; Wang, J.; Wu, Y.; Heremans, K. *Macromolecules* **2005**, *38*, 8923.
- (10) Mukae, K.; Sakurai, M.; Sawamura, S.; Makino, K.; Kim, S.; Ueda, I.; Shirahama, K. *J. Phys. Chem.* **1993**, *97*, 737.
- (11) Zhu, P. W.; Napper, D. H. *J. Colloid Interface Sci.* **1996**, *177*, 343.
- (12) Costa, R. O. R.; Freitas, R. F. S. *Polymer* **2002**, *43*, 5879.
- (13) Jung, S. C.; Oh, S. Y.; Chan Bae, Y. *Polymer* **2009**, *50*, 3370.
- (14) Zhu, P.; Napper, D. *Chem. Phys. Lett.* **1996**, *256*, 51.
- (15) Yamauchi, H.; Maeda, Y. *J. Phys. Chem. B* **2007**, *111*, 12964.
- (16) Dalkas, G.; Pagonis, K.; Bokias, G. *Polymer* **2006**, *47*, 243.
- (17) Pagonis, K.; Bokias, G. *Polym. Int.* **2006**, *55*, 1254.
- (18) Pagonis, K.; Bokias, G. *Polym. Bull.* **2007**, *58*, 289.
- (19) Winnik, F. M.; Ottaviani, M. F.; Bossmann, S. H.; Pan, W.; Garcia-Garibay, M.; Turro, N. J. *Macromolecules* **1993**, *26*, 4577.
- (20) Zhang, X. Z.; Chu, C. C. *Colloid Polym. Sci.* **2004**, *282*, 589.
- (21) Winnik, F. M.; Ringsdorf, H.; Venzmer, J. *Macromolecules* **1990**, *23*, 2415.
- (22) Schild, H. G.; Muthukumar, M.; Tirrell, D. A. *Macromolecules* **1991**, *24*, 948.
- (23) Winnik, F. M.; Ottaviani, M. F.; Bossmann, S. H.; Garcia-Garibay, M.; Turro, N. J. *Macromolecules* **1992**, *25*, 6007.
- (24) Zhang, G.; Wu, C. *Phys. Rev. Lett.* **2001**, *86*, 822.
- (25) Zhang, G.; Wu, C. *J. Am. Chem. Soc.* **2001**, *123*, 1376.

- (26) Shimizu, S.; Kurita, K.; Furusaka, M. *Appl. Phys. A: Mater. Sci. Process* **2002**, *74*, s389.
- (27) Tao, C.; Young, T. *Polymer* **2005**, *46*, 10077.
- (28) Tanaka, F.; Koga, T.; Winnik, F. *Phys. Rev. Lett.* **2008**, *101*, 28302.
- (29) Chen, J.-H.; Chen, H.-H.; Chang, Y.-X.; Chuang, P.-Y.; Hong, P.-D. *J. Appl. Polym. Sci.* **2008**, *107*, 2732.
- (30) Tanaka, F.; Koga, T.; Kojima, H.; Winnik, F. M. *Macromolecules* **2009**, *42*, 1321.
- (31) Pang, J.; Yang, H.; Ma, J.; Cheng, R. *J. Phys. Chem. B* **2010**, *114*, 8652.
- (32) Schild, H. G.; Tirrell, D. A. *J. Phys. Chem.* **1990**, *94*, 4352.
- (33) Hong, S.; Hong, P.; Chen, J.; Shih, K. *Eur. Polym. J.* **2009**, *45*, 1158.
- (34) Guettari, M.; Aschi, A.; Gomati, R.; Gharbi, A. *Mater. Sci. and Eng., C* **2008**, *28*, 811.
- (35) Guettari, M.; Gomati, R.; Gharbi, A. *J. Macromol. Sci., Part B* **2010**, *49*, 552.
- (36) Maeda, Y.; Nakamura, T.; Ikeda, I. *Macromolecules* **2002**, *35*, 217.
- (37) Berge, B.; Koningsveld, R.; Berghmans, H. *Macromolecules* **2004**, *37*, 8082.
- (38) Pagonis, K.; Bokias, G. *Polymer* **2004**, *45*, 2149.
- (39) Maeda, Y.; Sakamoto, J.; Wang, S.-y.; Mizuno, Y. *J. Phys. Chem. B* **2009**, *113*, 12456.
- (40) Bian, F. L.; Liu, M. Z.; Sheng, F. L. *Acta Phys. Chim. Sin.* **2004**, *20*, 337.
- (41) Panayiotou, M.; Garret-Flaudy, F.; Freitag, R. *Polymer* **2004**, *45*, 3055.
- (42) Amiya, T.; Hirokawa, Y.; Hirose, Y.; Li, Y.; Tanaka, T. *J. Chem. Phys.* **1987**, *86*, 2375.
- (43) Asano, M.; Winnik, F. M.; Yamashita, T.; Horie, K. *Macromolecules* **1995**, *28*, 5861.
- (44) Crowther, H.; Vincent, B. *Colloid Polym. Sci.* **1998**, *276*, 46.
- (45) Wang, N. A.; Ru, G. Y.; Wang, L. Y.; Feng, J. F. *Langmuir* **2009**, *25*, 5898.
- (46) López-León, T.; Bastos-González, D.; Ortega-Vinuesa, J. L.; Elaïssari, A. *ChemPhysChem* **2010**, *11*, 188.
- (47) Liu, G.; Zhang, G. *Langmuir* **2005**, *21*, 2086.
- (48) Pelton, R.; Richardson, R.; Cosgrove, T.; Ivkov, R. *Langmuir* **2001**, *17*, 5118.
- (49) Notley, S. M. *J. Phys. Chem. B* **2008**, *112*, 12650.
- (50) Brochard, F.; De Gennes, P. *Ferroelectrics* **1980**, *30*, 33.
- (51) Dixit, S.; Crain, J.; Poon, W.; Finney, J.; Soper, A. *Nature* **2002**, *416*, 829.
- (52) Guo, J.; Luo, Y.; Augustsson, A.; Kashtanov, S.; Rubensson, J.; Shuh, D.; Gren, H.; Nordgren, J. *Phys. Rev. Lett.* **2003**, *91*, 157401.
- (53) Koga, Y.; Nishikawa, K.; Westh, P. *J. Phys. Chem. A* **2004**, *108*, 3873.
- (54) Allison, S.; Fox, J.; Hargreaves, R.; Bates, S. *Phys. Rev. B* **2005**, *71*, 24201.
- (55) Liu, M.; Bian, F.; Sheng, F. *Eur. Polym. J.* **2005**, *41*, 283.
- (56) Katsumoto, Y.; Tanaka, T.; Ihara, K.; Koyama, M.; Ozaki, Y. *J. Phys. Chem. B* **2007**, *111*, 12730.
- (57) Shirota, H.; Kuwabara, N.; Ohkawa, K.; Horie, K. *J. Phys. Chem. B* **1999**, *103*, 10400.
- (58) Wang, X.; Wu, C. *Macromolecules* **1999**, *32*, 4299.
- (59) Vidyasagar, A.; Smith, H. L.; Majewski, J.; Toomey, R. G. *Soft Matter* **2009**, *5*, 4733.
- (60) Sun, S.; Hu, J.; Tang, H.; Wu, P. *J. Phys. Chem. B* **2010**, *114*, 9761.
- (61) Schmidt, P.; Dybal, J.; Trchová, M. *Vib. Spectrosc.* **2006**, *42*, 278.
- (62) Cheng, H.; Shen, L.; Wu, C. *Macromolecules* **2006**, *39*, 2325.
- (63) Corsaro, C.; Spooren, J.; Branca, C.; Leone, N.; Broccio, M.; Kim, C.; Chen, S.; Stanley, H.; Mallamace, F. *J. Phys. Chem. B* **2008**, *112*, 10449.
- (64) Nieto-Draghi, C.; Hargreaves, R.; Bates, S. *J. Phys.: Condens. Matter* **2005**, *17*, S3265.
- (65) Dougan, L.; Hargreaves, R.; Bates, S.; Finney, J.; Reat, V.; Soper, A.; Crain, J. *J. Chem. Phys.* **2005**, *122*, 174514.
- (66) Burba, C. M.; Carter, S. M.; Meyer, K. J.; Rice, C. V. *J. Phys. Chem. B* **2008**, *112*, 10399.
- (67) Thomas, M.; Richardson, H. H. *Vib. Spectrosc.* **2000**, *24*, 137.
- (68) Morita, S.; Shinzawa, H.; Noda, I.; Ozaki, Y. *Appl. Spectrosc.* **2006**, *60*, 398.
- (69) Noda, I. *Bull. Am. Phys. Soc.* **1986**, *31*, 520.
- (70) Noda, I. *J. Mol. Struct.* **2008**, *883–884*, 2.